Approximate attention with MLP: a pruning strategy for attention-based model in multivariate time series forecasting

Suhan Guo
School of Artificial Intelligence
Nanjing University
Nanjing
shguo@smail.nju.edu.cn

Jiahong Deng
School of Artificial Intelligence
Nanjing University
Nanjing
jiahongdeng@smail.nju.edu.cn

Yi Wei
School of Intelligence Science and Technology
Nanjing University
Nanjing
ywei@smail.nju.edu.cn

Hui Dou
Department of Computer Science and Technology
Nanjing University
Nanjing
huidou@smail.nju.edu.cn

Furao Shen*
School of Artificial Intelligence
Nanjing University
Nanjing
frshen@nju.edu.cn

Jian Zhao*
School of Electronic Science and Engineering
Nanjing University
Nanjing
jianzhao@nju.edu.cn

ABSTRACT

Attention-based architectures have become ubiquitous in time series forecasting tasks, including spatio-temporal (STF) and long-term time series forecasting (LTSF). Yet, our understanding of the reasons for their effectiveness remains limited. This work proposes a new way to understand self-attention networks: we have shown empirically that the entire attention mechanism in the encoder can be reduced to an MLP formed by feedforward, skip-connection, and layer normalization operations for temporal and/or spatial modeling in multivariate time series forecasting. Specifically, the Q, K, and V projection, the attention score calculation, the dot-product between the attention score and the V, and the final projection can be removed from the attention-based networks without significantly degrading the performance that the given network remains the top-tier compared to other SOTA methods. For spatio-temporal networks, the MLP-replace-attention network achieves a reduction in FLOPS of 62.579% with a loss in performance less than 2.5%; for LTSF, a reduction in FLOPs of 42.233% with a loss in performance less than 2%.

Keywords attention · spatio-temporal forecasting · long time series forecasting

1 Introduction

A time series consists of data points recorded chronologically at fixed intervals. By leveraging the temporal trends within historical data, we can predict future data points, a task known as time series forecasting. This task finds wide applications in real-world scenarios such as electricity consumption [1], infectious disease status [2], and stock market fluctuations [3], and traffic prediction [4]. Most applications' records can be formulated into a multivariate time series, considered a multi-channel signal. Depending on the background, the channels are referred to as the variables, nodes, or spatial dimensions. Based on assumptions of intern-channel dependencies, some studies propose to address channels

independently [5, 6, 7], while others model sensor correlations implicitly by projecting their input signal vector to the embedding space to mix information [8, 9, 10].

Denoting the lookback window and forecasting horizon to be $\mathcal{T}$ and $\mathcal{H}$, we summarize mainstream multivariate time series forecasting problems into the following two types:

- Long-term Time Series Forecasting (LTSF): to forecast a sequence that is much larger than the lookback window, denoted as $\mathcal{T} \ll \mathcal{H}$. No explicit requirement is solicited for model structure.
- Spatio-Temporal Forecasting (STF): to forecast a sequence that is at most as large as the lookback window, denoted as $\mathcal{T} \geq \mathcal{H}$. The model structure should explicitly model temporal and spatial dependencies.

In both tasks, the transformer-based structure is a popular backbone to model temporal and/or spatial dependencies. In particular, the attention mechanism addresses the associations between different time steps and/or channels.

Since time- and space-complexity is quadratic in the length of the input for attention, attention-based models for LTSF primarily focus on the possibility of reducing the computational cost of attention score from $\mathcal{O}(n^2)$ to $\mathcal{O}(n(\log n)^2)$ or even $\mathcal{O}(n)$ [11, 12]. However, it has been proven that under the Strong Exponential Time Hypothesis (SETH), as long as the attention score is calculated, the cost cannot be reduced to below $\mathcal{O}(n^2)$ theoretically [13]. Moreover, empirical evidence has shown that the simple linear transformation can outperform many transformer-based models in LTSF, rendering the attention mechanism a controversial module for temporal modeling [6]. Recent works have demonstrated that transformer-based models, with designs to reduce model complexity, can still outperform simple linear transformations in LTSF [7, 14]. However, these models are hardly cost-effective because the improvement in performance is not comparable to the addition of model parameters and computational cost.

Spatio-temporal data is a special type of multivariate time series that accentuates both spatial and temporal dependencies. Since the measurement at each location is closely related to its historical values as well as that of neighboring locations, it is vital to model both spatial and temporal dependencies explicitly with the network [15]. The documentation of many applications can be summarized into spatio-temporal data. One of the most commonly used scenarios is the traffic flow prediction because the flow at a road intersection is influenced by both the time of day and the upstream and downstream traffic. The proximity between sensors is often summarized in a geographic adjacency map where a larger weight is assigned to the edge between sensors closer to the Euclidean distance [16].

Following the tradition from two foundation works STGCN [17] and DCRNN [16], which defined the spatio-temporal forecasting task, researchers often address temporal and spatial dependencies differently. Temporal dependencies are modeled using CNN [18, 4], LSTM [16, 19], or attention mechanism [20, 21], while the spatial dependencies are viewed as a graph learning task. Because the geographic graph is insufficient to describe dependencies, a group of neural network models [18, 4, 22, 23] utilizes a graph mined from the data as the adjacency matrix for the downstream graph neural network module, referring to the graph as adaptive.

To reduce the computational cost, previous works' primary concern is pruning edges in either the spatial graph's adjacency matrices or the weight matrices in temporal modules via a sparsification algorithm [24, 25, 26, 27, 28]. By investigating the code and formula in some popular models, we notice that actual implementations for the traditional attention layers and the graph convolutional layers are closely related, as shown in section 3.3. Thus, we reduce the graph convolutional layers to a modified attention mechanism, as shown in Figure 1.

To investigate both LTSF and TSF problems, we define models using original and/or modified attention mechanisms in their encoder structure to solve multivariate time series forecasting problems as **a**ttention-based **m**ultivariate **t**ime **s**eries **f**orecasting **m**odels (AMTSFM). In this work, we propose empirically proving the following statement: **The attention mechanism for AMTSFM can be approximated using MLP containing the feedforward, the skip connection, and the layer normalization.** We limit our investigations to the attention-based LTSF and STF models, for they are the SOTA models for forecasting tasks, and our question of interest is within the attention module. We summarize two layers of motivation behind our work. For practical applications, pruning the attention module to MLP can significantly reduce the computational complexity and model storage, promoting model deployment on resource-constraint devices and extending datasets with many nodes. For research purposes, many SOTA works take the attention module for granted, and the ablation studies only showcase scenarios where the entire module is removed, but they do not confirm that the Q, K, V projection and the attention score matrices contribute as anticipated in multivariate time series forecasting. Keeping the accuracy drop marginal, we would like to demonstrate that besides the embedding of input features, the foundation modules in the AMTSFM are the MLP containing skip connection, the layer normalization, and the feedforward, rendering scaled dot-product representing the relationship between input time step or nodes to be redundant.

One of the most related works we can find is the work using adaptive graph sparsification to sparsify adaptive spatial-temporal graph neural networks [24]. Different from them, our focus is not on finding an optimal sparsification algorithm but on assessing the effectiveness of the attention weight matrices. Focusing mainly on attention-based
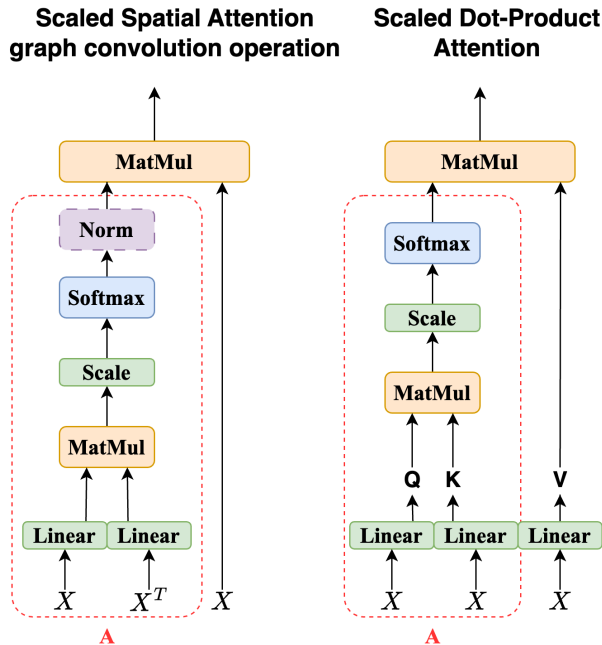
Figure 1: GCN is a modified version of the attention mechanism in code implementation.

networks, **we have discovered that these networks do not require spatial or temporal attention matrices for both training and inference stages** because only a minor drop in performance is observed with a significant drop in FLOPs. Our empirical results imply that LTSF and TSF require primarily the embedding and linear transformation of input features, rendering the explicit modeling of temporal and channel dependencies using the scaled dot-product attention less than optimal.

Our main contributions are summarised as follows:

- To the best of our knowledge, this is the first study on the effectiveness of attention modules in AMTSFM. By replacing the attention mechanism in attention-based spatio-temporal models with a simple translation (adding a bias term to the input feature), including STAEFormer and ASTGNN, we observe an average increase in MAE, RMSE, and MAPE by 2.107%, 2.052%, and 3.065% with an average FLOPs and parameters drop of 62.247% and 35.330%. Similarly, for LTSF, an average increase in MSE and MAE by 1.728% and 0.742% with a drop in FLOPs and parameters of 52.173% and 34.139% is also observed in non-traffic datasets using the PatchTST and iTransformer model.

- We have proposed an abstract structure for attention-based spatio-temporal networks by reducing the adaptive graph neural network to slightly modified attention. Based on the abstraction, we observe that removing both spatial and temporal attention modules, the module contributing the highest computational complexity, does not significantly deteriorate forecasting performance. The pruned model requires no pre-training or fine-tuning to retain decent inference performance.

- With further investigation, we discover that the attention in the decoder is much more significant than the attention in the encoder, which can be safely removed without degrading the performance. Replacing the attention mechanism with bias in the decoder module will cause a performance drop of 45.000%, 32.094%, and 54.184% in MAE, RMSE, and MAPE with FLOPs drop of 40.186% due to the greedy decoding strategy at the inference stage.

- We have empirically proven that among the MLP structure used to approximate the encoder attention, the skip connection is the core structure of AMTSFM, which means that the forecasting task using current multivariate datasets can be considered as a single variate forecasting task, ignoring the dependencies between time steps and nodes.

2 Related Work

2.1 Attention-Based Spatio-Temporal Traffic Flow Forecasting

Traffic flow forecasting is a critical task in intelligent transportation systems, requiring the effective capture of spatial and temporal dependencies within traffic data. In recent years, both GNN-based and Transformer-based methods have been extensively explored for this purpose. With the advent of GNNs, researchers have leveraged the graph messaging mechanism to model spatial dependencies and have enhanced forecasting accuracy by integrating both temporal and spatial features. GMAN [20] introduces spatial and temporal attention mechanisms to capture the dynamic spatial and non-linear temporal correlations in traffic data. To more effectively model the dynamics of traffic across both temporal and spatial dimensions, ASTGNN [21] incorporates an innovative temporal block based on multi-head self-attention, along with a novel dynamic graph convolution module. Notably, most GNN-based models employ attention mechanisms similar to those utilized in Transformer-based architectures. Despite their effectiveness, GNN-based models have limitations in traffic prediction. For instance, the spatial dependencies between locations are highly dynamic, and distant locations may exhibit similar traffic patterns. To address this, PDFormer [29] introduces a traffic delay-aware feature transformation module to model time delay and employs two graph masks to capture both short- and long-range spatial dependencies. Rather than designing complex models, STAEformer [30] proposes a novel spatio-temporal adaptive data embedding, applying it to the vanilla Transformer to achieve state-of-the-art (SOTA) performance. In this research, we explore both GNN-based and Transformer-based models, as their implementations are closely related.

2.2 Transformer-Based Long-term Time Series Forecasting

The Transformer architecture has emerged as one of the most popular frameworks for addressing sequence-related problems, including long-term time series forecasting. LogTrans [31] utilizes convolutional self-attention layers within a LogSparse Transformer to model local context and reduce space complexity, alleviating the memory bottleneck in standard Transformers. Informer [8] introduces a ProbSparse self-attention mechanism and a distillation operation to enhance predictive capacity while reducing time complexity and memory usage. Autoformer [9] proposes a novel decomposition architecture with an Auto-Correlation mechanism to capture dependencies at the series level. Pyraformer [10] incorporates a pyramidal attention module with an inter-scale tree structure and intra-scale neighboring connections, achieving linear complexity. FEDformer [32] introduces Fourier-enhanced blocks after seasonal-trend decomposition to achieve linear complexity. PatchTST [7] employs a channel-independent patch mechanism that segments the input sequence into subseries-level patches, used as input tokens for the Transformer, resulting in state-of-the-art forecasting accuracy. Most of these studies focus on optimizing time and space complexity by introducing novel attention-based mechanisms. In this paper, we investigate the necessity of attention mechanisms in long-term time series forecasting and compare the performance of Transformer-based models with and without these mechanisms.

2.3 Effective of Attention Mechanism

The core structure of the Transformer [33] is the self-attention mechanism, whose time and space complexity is quadratic to the input length, allowing it to capture dependencies between sequence elements. Previous research [13] has demonstrated that self-attention mechanisms inherently exhibit quadratic time complexity under the Strong Exponential Time Hypothesis and proposed a linear-time approximation method with exponential polynomial order dependence. Besides the computational cost, the effectiveness of self-attention has also been explored. The rank of neural networks measures information flowing across layers, and it is used as a tool to assess the effectiveness of model structures [34]. Assessing the rank of the network, it has been proven theoretically that skip connections and MLPs prevent the stacking of self-attention layers from degrading the network to rank-1 matrices, ensuring the expressiveness of attention-based architectures [35].

In addition to theoretical analysis of attention mechanisms, there are also some practical studies. Zeng et al. [6] challenge the effectiveness of Transformer-based models in long-term time series forecasting, demonstrating that a simple linear model, LTSF-Linear, outperforms complex Transformer models across multiple benchmarks, suggesting that the temporal modeling capabilities of Transformers in time series may be overestimated. Duan et al. [24] presents a method to localize Adaptive Spatial-Temporal Graph Neural Networks by sparsifying their spatial graph adjacency matrices, showing that while spatial dependencies are crucial for training, they can be largely disregarded during inference. In this paper, we focus on both spatial-temporal traffic flow forecasting and long-term time series forecasting, investigating the necessity of attention matrices in the attention module during both training and inference stages.

4

3 Methods

3.1 Definition of Multivariate Time Series Data Structure

The multivariate time series is defined as a sequence of discrete signal matrices $\mathcal{X} = \{X_{t-T}, \ldots, X_{t-1}\}$. Given the lookback window to be $T = \mathcal{T}$, we observe historical signals as $\mathcal{X} = \{X_{t-\mathcal{T}}, \ldots, X_{t-1}\} \in \mathbb{R}^{\mathcal{T} \times N \times C}$, where $X_t \in \mathbb{R}^{N \times C}$ represents a signal matrix at time t for N nodes with C features. Besides the signal matrix, the input data includes a network structure abstracted as a graph $\mathcal{G} = (\mathcal{V}, \mathcal{E})$ for STF. The graph $\mathcal{G}$ represents a network containing $|\mathcal{V}| = N$ nodes, which can be traffic detectors, observation stations, etc., and $|\mathcal{E}| = M$ edges, which describe the absence or weights of connections between node pairs. Defining the forecasting window as $\mathcal{H}$ and the learnable parameters as θ, we aim to learn the mapping $\mathcal{F}(\cdot; \theta)$, defined as:

$$\{X_t, \ldots, X_{t+\mathcal{H}}\} = \mathcal{F}(\mathcal{X}; \theta, \mathcal{G}). \tag{1}$$

For LTSF, the graph $\mathcal{G}$ has the following property:

$$\mathcal{E} \sim \text{Uniform}(\frac{1}{N}). \tag{2}$$

Since no prior information on variate dependencies is provided, the graph input is neglected for LTSF.

3.2 Modeling the Temporal Association

Attention is a core structure in a group of spatio-temporal models, which gathers the association between adjacent and non-adjacent positions in the sequence as weights and outputs a weighted sum. It has also been implemented with modifications to the LTSF models to model temporal dependencies efficiently. Multi-head attention consists of several layers running in parallel to attend to information from different representation subspaces at different positions. For each head, the self-attention score $S \in \mathbb{R}^{\mathcal{T} \times \mathcal{T}}$ is obtained from the dot-product between the query and key, denoted as $Q, K \in \mathbb{R}^{\mathcal{T} \times d_{\text{head}}}$, at the temporal dimension, which is shown as:

$$Q = E_n^{(l-1)} W^Q, \quad K = E_n^{(l-1)} W^K,$$
$$S = \text{softmax}(\frac{QK^T}{\sqrt{d_{\text{head}}}}). \tag{3}$$

The $E_n^{(l-1)} \in \mathbb{R}^{\mathcal{T} \times d_{\text{head}}}$ represents the input for the current module and the weighted sum is obtained using:

$$H = S(E_n^{(l-1)} W^V) = SV, \tag{4}$$

where $V \in \mathbb{R}^{\mathcal{T} \times d_{\text{head}}}$ is the value. The weighted sums from K heads are concatenated, denoted as $[\cdot]$, and projected with $W^O \in \mathbb{R}^{d_{\text{model}} \times d_{\text{model}}}$, shown as:

$$E_t^{(l)} = [H_1, \ldots, H_K] W^O. \tag{5}$$

Summarizing the above equations, we recapitulate the temporal module for attention-based models as follows:

$$E_n^{(l)} = \text{TemporalAttention}(E_n^{(l-1)}). \tag{6}$$

3.3 Modeling the Spatial Association

Geographical adjacency matrix $\mathcal{A}_s \in \mathbb{R}^{N \times N}$ and dynamic adjacency matrix $\mathcal{A}_d \in \mathbb{R}^{N \times N}$ are common ones for most spatio-temporal research. The geographical adjacency matrix is often available for traffic datasets where the distance between detectors is transformed into connection weights. However, the geographical adjacency matrix is not attainable for all datasets and does not adequately describe node relationships. Therefore, the dynamic adjacency matrix is proposed to represent the node dependencies, which is learned from the input node feature $Z_t^{(l-1)} \in \mathbb{R}^{N \times d_{\text{model}}}$, i.e.,

$$\mathcal{A}_d = \text{softmax}\left(\frac{(Z_t^{(l-1)} W^Q)(Z_t^{(l-1)} W^K)^T}{\sqrt{d_{\text{model}}}}\right). \tag{7}$$

The W^Q, W^K and W^V represent the learnable weights in linear projection layers. With an adjacency matrix, a Graph Convolutional Network (GCN) layer is defined as:

$$\tilde{\mathcal{A}} = D^{-\frac{1}{2}} \mathcal{A} D^{-\frac{1}{2}}, \tag{8}$$
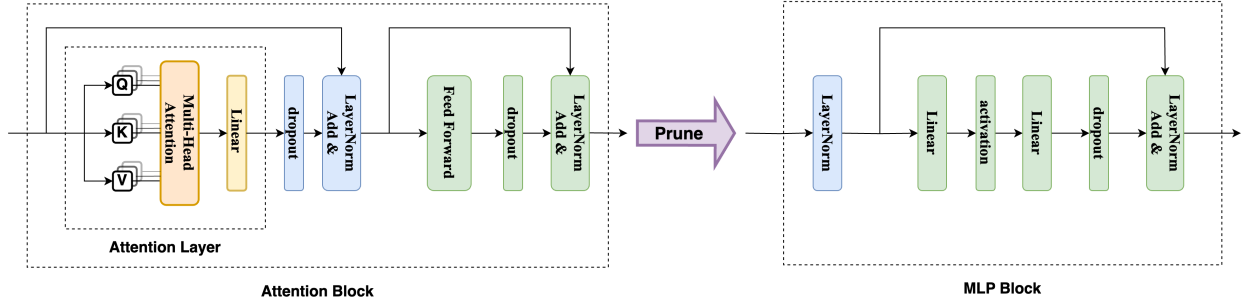$$Z_t^{(l)} = \sigma(\tilde{\mathcal{A}} Z_t^{(l-1)} \Theta), \tag{9}$$

Figure 2: Remove the attention layer in the attention block, which transforms the attention block to MLP block containing Feedforward, skip connection and layer normalization layers.

where $\mathcal{A}$ can be either a geographical or dynamic adjacency matrix and $\sigma(\cdot)$ represents the activation function.

In implementation, the GCN module is often reduced to slightly modified single-head attention applied to the node dimension. For the dynamic generation of the adjacency matrix, we observe that Eq. (7) is the same as the attention score generation shown in Eq. (3). For the message propagation stage, the matrix normalization, as shown in Eq. (8) is often omitted. As a result, the Eq. (9) is the same as Eq. (4) and Eq. (5), removing the value projection layer but adding an activation function.

For LTSF tasks, if the channel-mixing assumption is adopted, researchers model the spatial associations at the embedding layers without explicit GCN, as shown above. If channel independence is assumed, then variables are believed to be independent. However, some studies choose to focus on spatial dependencies, such as the iTransformer [?]. They propose an inverted attention layer, similar to our spatial attention structure, and the temporal association is modeled using the feed-forward layers.

In summary, the spatial module for attention-based models is:

$$Z_t^{(l)} = \text{SpatialAttention}(Z_t^{(l-1)}) \tag{10}$$

3.4 Abstract Structure of AMTSFM

Since both temporal and spatial associations are modeled using the attention mechanism in implementation, the spatio-temporal networks can be reduced to three components, including the embedding module, the encoder, and the decoder, as shown in Figure 2.

3.4.1 Embedding

The naive embedding layer is a linear projection that maps the raw input to the desired dimension. Some embedding layers added temporal patterns, such as the day-of-week and timestamps-of-day, with embedding layers. Some also embed the order of spatial dimension into a higher dimension and add to the input feature to improve the models' awareness of spatial connections. In general, the embedding layer can be summarized as:

$$E_0 = Embedding(X^t), \tag{11}$$

where input is mapped to feature $E_0 \in \mathbb{R}^{\mathcal{T} \times N \times d_{\text{model}}}$.

3.4.2 Encoder

The encoder consists of modules that model the spatial and temporal associations alternatively. Since multiplications between tensors are treated as batched matrix multiplication, we define a split and stack function as $\ominus(\cdot; D)$ and $\oplus(\cdot; D)$ respectively with D represents the assigned dimension. These functions are as follows:

$$\{E_{n=1}^{(0)}, \ldots, E_{n=N}^{(0)}\} = \ominus(E_0; N), \tag{12}$$

$$E_0 = \oplus(E_{n=1}^{(0)}, \ldots, E_{n=N}^{(0)}; N) \tag{13}$$

where temporal input $E_n^0 \in \mathbb{R}^{\mathcal{T} \times d_{\text{model}}}$ is obtained by spliting the input feature E_0 at the node dimension N. The $E_0 \in \mathbb{R}^{\mathcal{T} \times N \times d_{\text{model}}}$ represents the temporal outputs stacked at the node dimension.

To distinguish between TSF and LTSF, we define an indicator function as:

$$\mathbb{I}(\tau = 1), \tag{14}$$

where $\tau = 1$ and $\tau = 2$ represent TSF and LTSF, respectively. The modeling of spatial dependencies is default for TSF but optional for LTSF.

Defining the final output from the temporal module to be the input to the spatial module, denoted as $Z_0 = E_L$, the encoder is defined as:

$$E_L = \mathcal{O}_{l=1}^L \oplus (\text{TemporalAttention}_l(\ominus(E_0; N)); N), \tag{15}$$

$$Z_L = \mathcal{O}_{l=1}^L \oplus (\mathbb{I}(\tau = 1)\text{SpatialAttention}_l(\ominus(Z_0; T)); T), \tag{16}$$

where the $\mathcal{O}_{l=1}^L$ represents the function compositions. Notice that layer normalization, feed-forward projection, dropout, and residual connection are integrated between each attention module. We omit them in the above equation for clarity, and they are illustrated in the section **??**.

3.4.3 Decoder

Some studies adopt the original form for decoders, which employs a masked version of the attention module to ensure that the predictions can depend only on the known outputs at previous positions, denoted with $\delta = 1$. For other models, the decoder is replaced with a simple linear projection or convolutional layer to prevent overfitting, denoted as $\delta = 2$. Hence, we summarize the decoder into the following equation:

$$E_K = \mathcal{O}_{l=1}^K \oplus (\mathbb{I}(\delta = 1)\text{TemporalAttention}_l(\ominus(E_0; N)) + \mathbb{I}(\delta = 2)\text{TemporalProj}_l(\ominus(E_0; N)); N), \tag{17}$$

$$Z_K = \mathcal{O}_{l=1}^K \oplus (\mathbb{I}(\delta = 1)\text{SpatialAttention}_l(\ominus(Z_0; T)) + \mathbb{I}(\delta = 2)\text{SpatialProj}_l(\ominus(Z_0; T)); T), \tag{18}$$

3.5 Replace Attention with MLP

We remove the TemporalAttention($\cdot$) and SpatialAttention($\cdot$) modules while retaining the remaining operations in each attention block, we discover that the drop in performance is moderate while the decrease in FLOPs is considerable. Besides the core attention mechanism, there are auxiliary operations, including layer normalization, dropout, and residual connections. Taking the temporal module input $E_n^{(l-1)}$ as an example, these operations are organized as follows:

$$R_n^{(l)} = \text{LayerNorm}(\text{Dropout}(E_n^{(l-1)})) + E_n^{(l-1)}), \tag{19}$$

$$F_n^{(l)} = \sigma(R_n^{(l)} W^F) W^B, \tag{20}$$

$$E_n^{(l)} = \text{LayerNorm}(\text{Dropout}(F_n^{(l)}) + R_n^{(l)}). \tag{21}$$

$W^F \in \mathcal{R}^{d_{\text{model}} \times d_{\text{feedforward}}}$ and $W^B \in \mathcal{R}^{d_{\text{feedforward}} \times d_{\text{model}}}$ are two linear projection weights for the feedforward layers, which maps the current feature to higher dimension and back. We summarize the Eq. (19), Eq. (20) and Eq. (21) as:

$$E_n^{(l)} = \text{SkipNormFFN}(E_n^{(l-1)}), \tag{22}$$

$$Z_t^{(l)} = \text{SkipNormFFN}(Z_t^{(l-1)}), \tag{23}$$

for temporal and spatial modules, respectively. Then, the encoder can be reformulated as:

$$E_L = \mathcal{O}_{l=1}^L \oplus (\text{SkipNormFFN}_l(\ominus(E_0; N)); N), \tag{24}$$

$$Z_L = \mathcal{O}_{l=1}^L \oplus (\mathbb{I}(\tau = 1)\text{SkipNormFFN}_l(\ominus(Z_0; T)); T). \tag{25}$$

Notice that the original computation cost is $\mathcal{O}(n^2)$ considering that the dimension of features maps is much smaller than number of nodes or sequence lengths. The bias-replace-attention version has a computation cost of $\mathcal{O}(d_{\text{model}})$, which removes the quadratic dependency on the sequence length.

4 Experiments

We conduct the following experiments to demonstrate that 1) both spatial and temporal attention mechanisms can be eliminated without severely damaging performance for STF; 2) attention modules are not essential to represent temporal dependencies for LTSF.

4.1 Baseline models

We have selected two popular attention-based spatio-temporal network structures published recently, including the ASTGNN [21] and STAEFormer [30]. For LTSF, we have selected an attention-based SOTA model: PatchTST [7] and iTransformer [14]. Their primary features are summarized below:

- **ASTGNN**: Periodicity of traffic data and spatial heterogeneity are considered with global/local periodic tensor and spatial positional embedding. Both spatial and temporal correlations are obtained with the self-attention mechanism.
- **STAEformer**: A novel spatio-temporal adaptive embedding is proposed to capture intricate spatio-temporal relation in addition to the temporal periodicity embedding and feature embedding.
- **PatchTST**: Introducing channel independence to reduce multivariate times series to single variate and segmenting time series input into subseries-level patches to reduce computational cost.
- **iTransformer**: Application of attention on the spatial dimension and feedforward in the temporal dimension to capture multivariate correlations and nonlinearity.

4.2 Datasets

The mlp-replace-attention models are evaluated in real-world spatio-temporal datasets, including METR-LA, PEMS-Bay, PEMS04, PEMS07 and PEMS08. DCRNN [16] proposed the first two datasets and the rest were proposed by STSGCN [22]. For long-term time series forecasting, we use 8 popular multivariate datasets to evaluate the performance [7]. Detailed statistics are in Table 1.

Table 1: Dataset Statistics

	STF							
Datasets	METR-LA	PEMS-Bay	PEMS04	PEMS07	PEMS08			
Nodes	207	325	307	883	170			
Time Steps	34,272	52,116	16,992	28,224	17,856			
Time Range	03/2012-06/2012	01/2017-05/2017	01/2018-02/2018	05/2017-08/2017	07/2016-08/2016			
	LTSF							
Datasets	Weather	Traffic	Electricity	ILI	ETTh1	ETTh2	ETTm1	ETTm2
Nodes	21	862	321	7	7	7	7	7
Time Steps	52,696	17,544	26,304	966	17,420	17,420	69,680	69,680

4.2.1 Traffic

The METR-LA and PEMS-BAY datasets are split with 70% for training, 10% for validation, and 20% for testing. We use the past 1-hour (12 steps) data to predict the traffic flow for the next 15-min (3 steps), 30-min (6 steps), and 1 hour (12 steps). To be consistent with previous works, the point estimate of metrics for the three prediction lengths is reported, i.e., the metrics at steps 3, 6, and 12 are reported from the 1-hour forecasting task. We also added an "average" estimate, the mean over the 1-hour forecasting. For PEMS04, PEMS07, and PEMS08, we split the data with 60% for training, 20% for validation, and 20% for testing to be consistent with most modern methods. We use the past 12 steps to predict the 12 steps forward, and averaged metrics are reported. To limit the focus of the study to the attention mechanism, networks are trained with their original versions of data normalization and embedding.

4.2.2 Non-traffic

We strictly follow the standard protocol from previous works for dataset splitting, in which we divide all datasets into training, validation, and test sets in chronological order. For the ETT datasets, we use a split ratio of $6:2:2$, while for other datasets, we adopt a ratio of $7:1:2$. For the illness dataset, the lookback window is set to be 36, and the forecasting horizon is $24, 36, 48,$ and 60. For the other datasets, the lookback window is 96, and the forecasting horizon is $96, 192, 336,$ and 720.

4.3 Setting and metrics

Experiments are conducted on a machine with eight NVIDIA GeForce RTX 2080 GPUs. All networks are implemented with Ubuntu 18.04. To ensure the best performance, we follow the loss function, Pytorch, and Python version as

in the original paper. For the traffic dataset, the evaluation metrics include mean absolute error (MAE), root mean squared error (RMSE), and mean absolute percentage error (MAPE). For evaluation, all MAPE results are reported as a percentage by comparing the predicted data re-transformed to the original scale and the ground truth. As done by baselines, MAE and RMSE are reported using the re-transformed original-scale prediction for the traffic dataset. Missing values are excluded from training and inference. For non-traffic datasets, MAE and RMSE are reported as in the original paper. The computational cost is measured in FLOPS (FLoating-point Operations Per Second), and the model storage is represented in G (Gigabytes). We repeat all experiments five times and report the average results.

4.4 Results

We summarize our major experiments using spatio-temporal data in section 4.4.1 and multivariate data in section 4.4.2. To validate our main argument, we first train the selected networks using their corresponding datasets to obtain baseline metrics. Then, we replace all the attention modules in the encoder structure with an MLP and re-run the same experiments with the same experimental settings. For MAE, RMSE, and MAPE metrics, the standard deviation from five runs is included. The FLOPS($\downarrow$) compares the inference FLOPS bias-replace-attention model with the original model and represents the decrease with a percentage. The Params($\downarrow$) showcase the difference in parameters between the original model and the MLP-replace-attention model.

4.4.1 Traffic

Table 2: Performance of STAEformer for traffic datasets. The three columns represent the original model, the MLP-replace-attention model, and the improvement between the two. MAE, RMSE, and MAPE improvements are indicated in bold font.

STAEformer		Original Model			MLP-replace-attention			Improvement				
		MAE	RMSE	MAPE(%)	MAE	RMSE	MAPE(%)	MAE(↑)	RMSE(↑)	MAPE(↑)	FLOPS(↓)	Params(↓)
PEMS04	Avg.	18.229 ± 0.032	30.239 ± 0.114	12.047 ± 0.038	18.467 ± 0.015	30.19 ± 0.027	12.115 ± 0.025	1.307%	0.162%	0.566%	64.067%	41.193%
PEMS07	Avg.	19.234 ± 0.067	32.75 ± 0.138	8.061 ± 0.037	19.718 ± 0.044	33.463 ± 0.128	8.224 ± 0.033	2.517%	2.176%	2.022%	74.299%	29.252%
PEMS08	Avg.	13.479 ± 0.015	23.276 ± 0.068	8.854 ± 0.017	13.686 ± 0.041	23.365 ± 0.131	9.052 ± 0.034	1.536%	0.385%	2.242%	60.309%	45.622%
METR-LA	15min	2.656 ± 0.013	5.119 ± 0.051	6.898 ± 0.045	2.823 ± 0.004	5.58 ± 0.014	7.718 ± 0.032	6.282%	8.998%	11.883%	61.399%	44.334%
	30min	2.967 ± 0.018	6.023 ± 0.06	8.153 ± 0.078	3.184 ± 0.003	6.631 ± 0.015	9.361 ± 0.04	7.293%	10.097%	14.825%		
	60min	3.34 ± 0.014	7.023 ± 0.047	9.741 ± 0.092	3.546 ± 0.002	7.595 ± 0.009	10.943 ± 0.043	6.160%	8.146%	12.339%		
	Avg.	2.939 ± 0.014	5.989 ± 0.05	8.08 ± 0.067	3.126 ± 0.002	6.526 ± 0.013	9.129 ± 0.036	6.379%	8.961%	12.980%		
PEMS-BAY	15min	1.302 ± 0.003	2.774 ± 0.005	2.748 ± 0.016	1.356 ± 0.002	2.884 ± 0.014	2.884 ± 0.009	4.134%	3.971%	4.931%	64.509%	40.675%
	30min	1.603 ± 0.005	3.667 ± 0.011	3.606 ± 0.038	1.678 ± 0.002	3.811 ± 0.009	3.819 ± 0.008	4.664%	3.935%	5.915%		
	60min	1.865 ± 0.011	4.312 ± 0.019	4.376 ± 0.073	1.95 ± 0.002	4.476 ± 0.005	4.591 ± 0.004	4.548%	3.813%	4.929%		
	Avg.	1.539 ± 0.004	3.55 ± 0.014	3.449 ± 0.034	1.608 ± 0.002	3.693 ± 0.008	3.637 ± 0.005	4.482%	4.034%	5.437%		

Table 3: Performance of ASTGNN for traffic datasets. The three columns represent the original model, the MLP-replace-attention model, and the improvement between the two. MAE, RMSE, and MAPE improvements are indicated in bold font.

ASTGNN		Original Model			MLP-replace-attention			Improvement				
		MAE	RMSE	MAPE(%)	MAE	RMSE	MAPE(%)	MAE(↑)	RMSE(↑)	MAPE(↑)	FLOPS(↓)	Params(↓)
PEMS04	Avg.	18.492 ± 0.055	31.168 ± 0.226	12.406 ± 0.043	18.49 ± 0.038	31.002 ± 0.196	12.428 ± 0.084	**-0.011%**	-0.533%	0.177%	53.542%	31.492%
PEMS07	Avg.	18.34 ± 0.089	32.04 ± 0.167	7.668 ± 0.044	18.714 ± 0.068	32.928 ± 0.124	7.824 ± 0.027	2.039%	2.772%	2.034%	66.133%	25.465%
PEMS08	Avg.	12.79 ± 0.07	22.634 ± 0.079	8.712 ± 0.082	12.958 ± 0.073	22.972 ± 0.14	8.896 ± 0.212	1.314%	1.493%	2.112%	57.869%	32.128%
METR-LA	15min	3.306 ± 0.015	9.164 ± 0.038	7.508 ± 0.07	3.326 ± 0.008	9.128 ± 0.024	7.626 ± 0.073	0.605%	**-0.393%**	1.572%	58.795%	31.803%
	30min	4.308 ± 0.017	11.656 ± 0.031	9.572 ± 0.14	4.328 ± 0.017	11.614 ± 0.033	9.668 ± 0.075	0.464%	**-0.360%**	1.003%		
	60min	5.626 ± 0.022	14.39 ± 0.055	12.152 ± 0.206	5.698 ± 0.035	14.436 ± 0.037	12.254 ± 0.12	1.280%	0.320%	0.839%		
	Avg.	4.264 ± 0.014	11.624 ± 0.029	9.444 ± 0.13	4.302 ± 0.02	11.63 ± 0.021	9.55 ± 0.075	0.891%	0.052%	1.122%		
PEMS-BAY	15min	1.298 ± 0.004	2.844 ± 0.008	2.752 ± 0.027	1.3 ± 0.006	2.84 ± 0.017	2.726 ± 0.021	0.154%	**-0.141%**	**-0.945%**	61.151%	31.339%
	30min	1.61 ± 0.009	3.816 ± 0.022	3.718 ± 0.044	1.612 ± 0.007	3.79 ± 0.028	3.674 ± 0.042	0.124%	**-0.681%**	**-1.183%**		
	60min	1.882 ± 0.01	4.548 ± 0.038	4.586 ± 0.057	1.876 ± 0.01	4.502 ± 0.037	4.486 ± 0.051	**-0.319%**	**-1.011%**	**-2.181%**		
	Avg.	1.544 ± 0.008	3.714 ± 0.025	3.554 ± 0.041	1.548 ± 0.007	3.69 ± 0.024	3.508 ± 0.034	0.259%	**-0.646%**	**-1.294%**		

Employing traffic datasets, we observe that replacing the attention module with the MLP causes a marginal drop in forecasting performance but a major decrease in inference speed. STAEformer consists of vanilla transformer encoder blocks, and an average MAE, RMSE, and MAPE drop of $3.244\%, 3.331\%,$ and 4.981%, and a FLOPS decrease of 65.135% is observed in Table 2. ASTGNN bears an original encoder-decoder structure, and the results are shown in Table 3. By removing the attention blocks in the encoder structure, we observe an average drop of 0.970%, 0.773%, and 1.148% in MAE, RMSE, and MAPE and a FLOPS drop of 59.360%. We notice that for ASTGNN, it seems that removing the attention modules promotes the performance of METR-LA and PEMS-BAY datasets, showing that stacking of attention modules can cause overfitting and deteriorate performance. From these two models, we conclude that reducing more than half of the computational cost without losing more than 2.5% of performance demonstrates that Q, K, and V projection and attention mapping are not essential to model spatio-temporal data. Comparing STAEFormer

Table 4: Performance of PatchTST for non-traffic datasets. The three columns represent the original model, the MLP-replace-attention model, and the improvement between the two. MAE and RMSE improvements are indicated in bold font.

PatchTST/42		Origin		MLP-replace-attention		Improvement			
		MSE	MAE	MSE	MAE	MSE(↑)	MAE(↑)	FLOPS(↓)	Params(↓)
Weather	96	0.151 ± 0.0005	0.199 ± 0.0003	0.158 ± 0.0003	0.204 ± 0.0002	4.558%	2.815%	52.011%	21.468%
	192	0.196 ± 0.0003	0.242 ± 0.0004	0.202 ± 0.0008	0.245 ± 0.0005	3.140%	1.262%	50.604%	13.761%
	336	0.248 ± 0.0006	0.283 ± 0.0008	0.252 ± 0.0004	0.283 ± 0.0003	1.364%	0.113%	48.631%	8.943%
	720	0.32 ± 0.0008	0.335 ± 0.0006	0.321 ± 0.0004	0.333 ± 0.0003	0.248%	**-0.412%**	44.050%	4.623%
Traffic	96	0.367 ± 0.0003	0.25 ± 0.0002	0.386 ± 0.0001	0.263 ± 0.0002	5.443%	4.893%	52.011%	21.468%
	192	0.386 ± 0.0006	0.259 ± 0.001	0.401 ± 0.0005	0.268 ± 0.001	4.047%	3.632%	50.604%	13.761%
	336	0.398 ± 0.0004	0.265 ± 0.0005	0.413 ± 0.0001	0.274 ± 0.0001	3.874%	3.414%	48.631%	8.943%
	720	0.433 ± 0.0013	0.286 ± 0.0022	0.443 ± 0.0007	0.293 ± 0.0012	2.294%	2.309%	44.050%	4.623%
Electricity	96	0.13 ± 0.0003	0.223 ± 0.0001	0.135 ± 0.0001	0.229 ± 0.0002	3.353%	2.468%	52.011%	21.468%
	192	0.148 ± 0.0003	0.24 ± 0.0005	0.149 ± 0.0001	0.243 ± 0.0001	0.725%	0.962%	50.604%	13.761%
	336	0.165 ± 0.0004	0.258 ± 0.0004	0.165 ± 0.0006	0.26 ± 0.0008	0.334%	0.721%	48.631%	8.943%
	720	0.203 ± 0.0008	0.293 ± 0.0009	0.207 ± 0.0006	0.296 ± 0.0004	1.957%	1.144%	44.050%	4.623%
ILI	24	1.565 ± 0.0974	0.824 ± 0.0237	1.538 ± 0.1079	0.833 ± 0.0272	**-0.339%**	1.192%	35.536%	9.629%
	36	1.478 ± 0.1269	0.837 ± 0.05	1.555 ± 0.1053	0.853 ± 0.0477	3.534%	1.439%	35.210%	7.754%
	48	1.782 ± 0.0696	0.915 ± 0.0273	1.833 ± 0.1028	0.918 ± 0.0583	4.016%	1.103%	34.889%	6.490%
	60	1.522 ± 0.2466	0.845 ± 0.0841	1.766 ± 0.1905	0.914 ± 0.0436	14.900%	7.448%	34.574%	5.581%
ETTh1	96	0.376 ± 0.0009	0.4 ± 0.0007	0.378 ± 0.0025	0.402 ± 0.0024	0.506%	0.508%	33.859%	3.935%
	192	0.413 ± 0.0014	0.421 ± 0.0011	0.415 ± 0.0024	0.422 ± 0.0024	0.413%	0.254%	31.623%	2.198%
	336	0.427 ± 0.0033	0.433 ± 0.0033	0.427 ± 0.002	0.43 ± 0.0021	**-0.078%**	**-0.758%**	28.773%	1.322%
	720	0.446 ± 0.0067	0.464 ± 0.0053	0.444 ± 0.0045	0.458 ± 0.003	**-0.510%**	**-1.255%**	23.201%	0.641%
ETTh1	96	0.376 ± 0.0009	0.4 ± 0.0007	0.378 ± 0.0025	0.402 ± 0.0024	0.436%	0.450%	33.859%	3.935%
	192	0.413 ± 0.0014	0.421 ± 0.0011	0.415 ± 0.0024	0.422 ± 0.0024	0.388%	0.233%	31.623%	2.198%
	336	0.427 ± 0.0033	0.433 ± 0.0033	0.427 ± 0.002	0.43 ± 0.0021	**-0.071%**	**-0.750%**	28.773%	1.322%
	720	0.446 ± 0.0067	0.464 ± 0.0053	0.444 ± 0.0045	0.458 ± 0.003	**-0.465%**	**-1.257%**	23.201%	0.641%
ETTh2	96	0.275 ± 0.0002	0.336 ± 0.0005	0.277 ± 0.0007	0.338 ± 0.0007	0.631%	0.515%	33.859%	3.935%
	192	0.339 ± 0.0011	0.378 ± 0.0012	0.34 ± 0.0008	0.381 ± 0.0007	0.203%	0.773%	31.623%	2.198%
	336	0.328 ± 0.0023	0.381 ± 0.0022	0.331 ± 0.0016	0.387 ± 0.0012	0.808%	1.543%	28.773%	1.322%
	720	0.378 ± 0.0012	0.421 ± 0.0014	0.383 ± 0.0015	0.425 ± 0.0009	1.015%	0.762%	23.201%	0.641%
ETTm1	96	0.29 ± 0.0017	0.342 ± 0.0006	0.292 ± 0.0022	0.346 ± 0.0014	0.988%	1.388%	52.011%	21.468%
	192	0.334 ± 0.0026	0.37 ± 0.001	0.334 ± 0.0008	0.373 ± 0.0006	0.054%	0.755%	50.604%	13.761%
	336	0.366 ± 0.0011	0.391 ± 0.0008	0.37 ± 0.0042	0.398 ± 0.0041	0.687%	1.344%	48.631%	8.943%
	720	0.417 ± 0.0022	0.423 ± 0.0014	0.414 ± 0.0026	0.422 ± 0.003	**-0.694%**	**-0.157%**	44.050%	4.623%
ETTm2	96	0.165 ± 0.001	0.254 ± 0.0004	0.165 ± 0.0006	0.255 ± 0.0005	**-0.045%**	0.550%	52.011%	21.468%
	192	0.221 ± 0.0009	0.292 ± 0.0008	0.223 ± 0.0004	0.295 ± 0.0005	0.969%	0.718%	50.604%	13.761%
	336	0.276 ± 0.0014	0.329 ± 0.001	0.279 ± 0.0018	0.331 ± 0.0011	0.793%	0.372%	48.631%	8.943%
	720	0.364 ± 0.0004	0.383 ± 0.0004	0.363 ± 0.0018	0.384 ± 0.0021	**-0.435%**	0.405%	44.050%	4.623%

to ASTGNN, we observe that the parameter drop is more significant in the STAEFormer structure because ASTGNN possesses an attention-based decoder structure.

4.4.2 Non-Traffic

We verify the effect of MLP-replace-attention models on the PatchTST model using non-traffic datasets. For MSE and MAE metrics, we observe a 1.835%, and 1.317% increase with an average decrease in FLOPS and Parameters by 42.238%, and 9.051%. Since the attention mechanism is correlated with the input size quadratically, the reduction in FLOPS also varies with the input size. Replacing the attention mechanism with an MLP improves performance for longer output lengths for Weather and ETT datasets, demonstrating that for these applications, an attention module is redundant in the network structure in modeling temporal correlation. PatchTST uses the patching technique to reduce the input size to the number of patches, 42, in our case, which already reduces the computational cost of the attention module. Our results demonstrate that the attention module can be further lightened without damaging the performance significantly.

Similar results are also observed for iTransformer structure that the MSE and MAE have a minor increase of 1.622% and 0.168%, with a major drop in FLOPs and parameters as 62.107% and 59.228%. We notice that removing the attention mechanism in iTransformer for ETT datasets results in a promoted performance with a significant decrease in inference cost. This can be attributed to the fact that ETT datasets have merely 7 nodes, so the correlation between

Table 5: Performance of iTransformer for non-traffic datasets. The three columns represent the original model, the MLP-replace-attention model, and the improvement between the two. MAE and RMSE improvements are indicated in bold font.

iTransformer		Origin		MLP-replace-attention		Improvement			
		MSE	MAE	MSE	MAE	MSE(↑)	MAE(↑)	FLOPS(↓)	Params(↓)
Weather	96	0.176 ± 0.0012	0.216 ± 0.002	0.183 ± 0.0005	0.221 ± 0.0005	4.020%	2.403%	65.709%	65.171%
	192	0.224 ± 0.0014	0.257 ± 0.0009	0.23 ± 0.0004	0.261 ± 0.0005	2.425%	1.405%	65.058%	64.514%
	336	0.282 ± 0.0019	0.299 ± 0.0014	0.285 ± 0.0002	0.3 ± 0.0001	0.923%	0.288%	64.103%	63.553%
	720	0.358 ± 0.0016	0.35 ± 0.0011	0.361 ± 0.0002	0.35 ± 0.0004	0.734%	**-0.042%**	61.691%	61.123%
Traffic	96	0.393 ± 0.0005	0.268 ± 0.0003	0.437 ± 0.0003	0.282 ± 0.0001	11.100%	5.211%	77.802%	65.511%
	192	0.413 ± 0.0003	0.277 ± 0.0003	0.449 ± 0.0002	0.287 ± 0.0002	8.789%	3.454%	77.419%	65.011%
	336	0.425 ± 0.0007	0.283 ± 0.0005	0.464 ± 0.0002	0.293 ± 0.0003	9.048%	3.566%	76.853%	64.277%
	720	0.458 ± 0.0013	0.301 ± 0.0004	0.495 ± 0.0002	0.312 ± 0.0002	8.138%	3.828%	75.381%	62.396%
Electricity	96	0.148 ± 0.0003	0.24 ± 0.0003	0.169 ± 0.0001	0.253 ± 0.0001	13.783%	5.326%	65.652%	58.549%
	192	0.164 ± 0.0008	0.255 ± 0.0008	0.177 ± 0.0001	0.261 ± 0.0001	7.788%	2.321%	69.285%	63.001%
	336	0.179 ± 0.0007	0.271 ± 0.0006	0.193 ± 0.0002	0.278 ± 0.0001	8.376%	2.601%	70.905%	65.043%
	720	0.214 ± 0.0069	0.302 ± 0.0047	0.234 ± 0.0005	0.312 ± 0.0004	9.331%	3.325%	72.636%	67.334%
ILI	24	2.329 ± 0.0427	1.041 ± 0.0156	2.384 ± 0.0211	1.057 ± 0.0049	2.374%	1.535%	64.359%	63.886%
	36	2.238 ± 0.0306	1.018 ± 0.0096	2.292 ± 0.0325	1.036 ± 0.0093	2.438%	1.732%	64.123%	63.648%
	48	2.063 ± 0.0761	0.989 ± 0.0287	2.052 ± 0.0209	0.976 ± 0.0056	**-0.557%**	**-1.323%**	65.233%	64.996%
	60	2.104 ± 0.0214	1.016 ± 0.0111	2.036 ± 0.0182	0.991 ± 0.0047	**-3.247%**	**-2.520%**	65.110%	64.873%
ETTh1	96	0.388 ± 0.0015	0.406 ± 0.0009	0.384 ± 0.0003	0.399 ± 0.0003	**-1.078%**	**-1.542%**	62.965%	62.482%
	192	0.444 ± 0.0009	0.438 ± 0.001	0.436 ± 0.0004	0.429 ± 0.0004	**-1.753%**	**-1.983%**	61.196%	60.702%
	336	0.488 ± 0.0018	0.459 ± 0.0014	0.475 ± 0.0006	0.448 ± 0.0005	**-2.650%**	**-2.418%**	62.401%	62.155%
	720	0.518 ± 0.0088	0.498 ± 0.0056	0.493 ± 0.0073	0.481 ± 0.0049	**-4.805%**	**-3.418%**	58.989%	58.730%
ETTh2	96	0.301 ± 0.0014	0.351 ± 0.0008	0.296 ± 0.0006	0.348 ± 0.0003	**-1.470%**	**-0.791%**	59.782%	58.798%
	192	0.379 ± 0.0007	0.399 ± 0.0007	0.377 ± 0.0011	0.397 ± 0.0005	**-0.627%**	**-0.384%**	56.733%	55.721%
	336	0.424 ± 0.0024	0.432 ± 0.001	0.419 ± 0.0003	0.431 ± 0.0002	**-1.142%**	**-0.229%**	52.702%	51.665%
	720	0.43 ± 0.0053	0.447 ± 0.003	0.426 ± 0.0003	0.445 ± 0.0002	**-1.033%**	**-0.599%**	44.306%	43.266%
ETTm1	96	0.343 ± 0.0013	0.377 ± 0.0009	0.332 ± 0.0026	0.367 ± 0.0014	**-2.938%**	**-2.526%**	59.782%	58.798%
	192	0.381 ± 0.0015	0.395 ± 0.001	0.373 ± 0.0003	0.386 ± 0.0003	**-2.122%**	**-2.253%**	56.733%	55.721%
	336	0.419 ± 0.0013	0.418 ± 0.0006	0.407 ± 0.0003	0.406 ± 0.0005	**-2.874%**	**-2.794%**	52.702%	51.665%
	720	0.491 ± 0.0025	0.458 ± 0.0013	0.469 ± 0.0003	0.441 ± 0.0003	**-4.431%**	**-3.709%**	44.306%	43.266%
ETTm2	96	0.185 ± 0.0006	0.271 ± 0.0012	0.182 ± 0.0002	0.266 ± 0.0003	**-1.863%**	**-1.555%**	59.782%	58.798%
	192	0.252 ± 0.001	0.313 ± 0.0006	0.247 ± 0.0003	0.308 ± 0.0003	**-1.748%**	**-1.481%**	56.733%	55.721%
	336	0.314 ± 0.001	0.351 ± 0.0004	0.308 ± 0.0003	0.347 ± 0.0001	**-1.820%**	**-1.255%**	52.702%	51.665%
	720	0.412 ± 0.0012	0.406 ± 0.0009	0.407 ± 0.0009	0.402 ± 0.0005	**-1.192%**	**-0.801%**	44.306%	43.266%

nodes may be neglected without significantly affecting the performance. In general, replacing the attention layer with the MLP layer retains the performance for LTSF tasks, showing that attention is not essential for the task.

4.5 Ablation Studies

To fully understand the contribution of attention mechanisms in different modules, we conduct ablations studies comparing the difference in attention replacement between spatial and temporal attention and between encoder and decoder.

4.5.1 Replace Spatial vs. Replace Temporal

For spatio-temporal networks using traffic datasets PEMS04, 07, and 08, we discover that removing the temporal attention leads to more performance drop than removing the spatial attention. However, removing spatial attention contributes more to the drop in FLOPs, demonstrating that spatial attention is not an essential building block for completing the forecasting task for these datasets. As shown in Figure 3, an average increase in MAE, RMSE, and MAPE of $1.904\%, 1.876\%$, and 1.813% are observed removing temporal attention and $0.453\%, 0.269\%$, and 0.417% spatial attention. FLOPs drop by 22.441%, and 40.147% are observed for temporal and spatial attention.

4.5.2 Replace Decoder vs. Replace Encoder

Since ASTGNN is the only model containing an attention-based decoder structure, we conduct the attention replacement experiment using it. Figure 4 shows the results. Removing decoder attention causes a significant performance drop that $45.000\%, 32.094\%$, and 54.184% increase is observed in MAE, RMSE, and MAPE. The removal of decoder attention
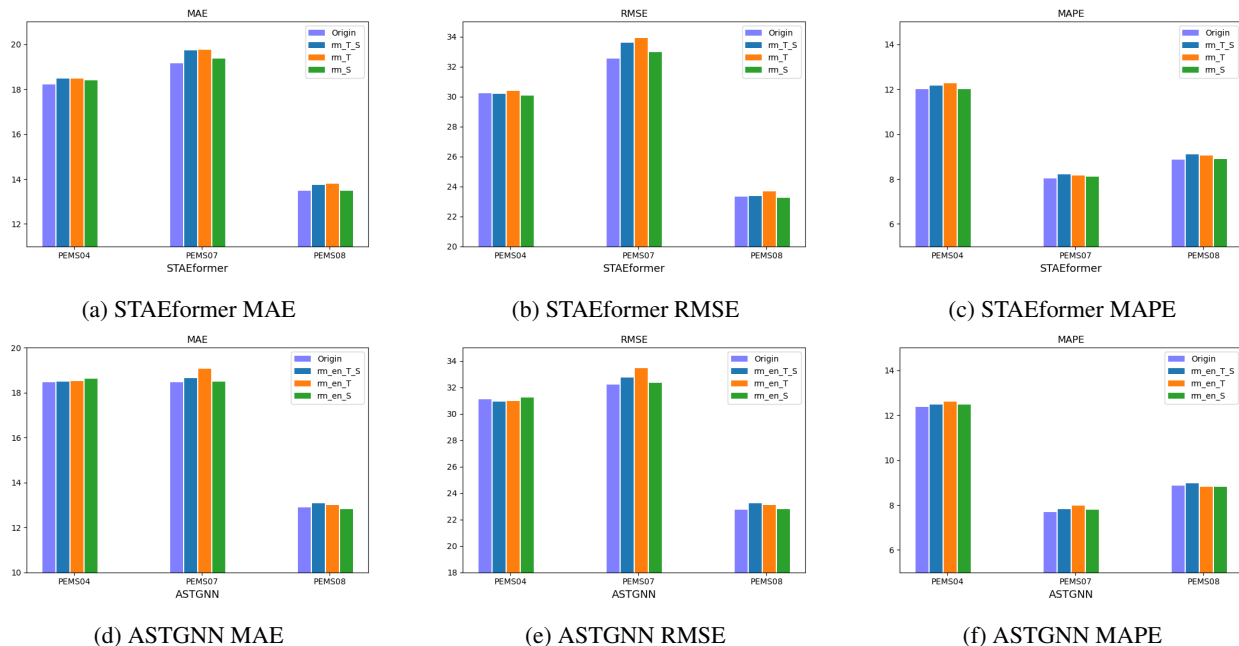
Approximate attention with MLP

(a) STAEformer MAE   (b) STAEformer RMSE   (c) STAEformer MAPE

(d) ASTGNN MAE   (e) ASTGNN RMSE   (f) ASTGNN MAPE

Figure 3: Performance comparison between replacing spatial and temporal attention layer with MLP layer on PEMS04, 07, 08 datasets.

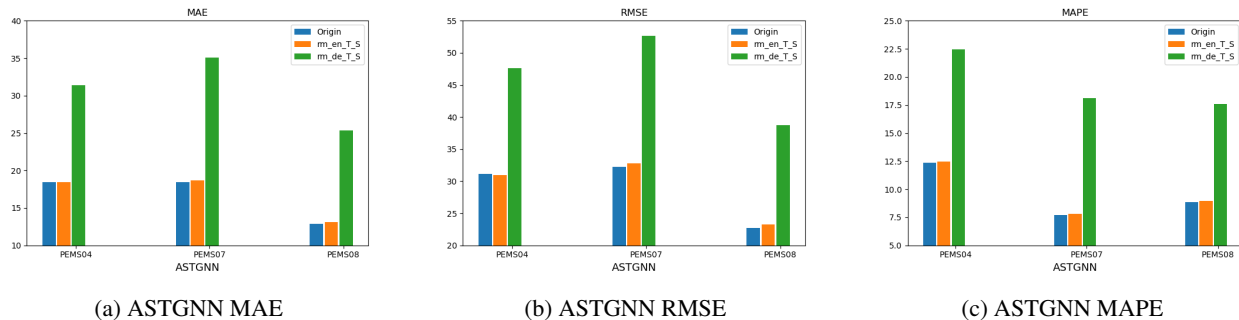(a) ASTGNN MAE   (b) ASTGNN RMSE   (c) ASTGNN MAPE

Figure 4: Performance comparison between replacing encoder and decoder attention layer with MLP layer on PEMS 04, 07, 08 datasets.

also causes a considerable FLOPS drop of 40.186%, which is a little less than the encoder attention contributed FLOPS drop of 59.360%. The inference of ASTGNN utilizes a greedy decoding strategy, and removing decoder attention renders it useless because the increment in decoder input will not lead to a parameter change, as does the scaled dot-product attention.

5 Conclusion

In this work, we have found that for spatio-temporal and long-term time series forecasting tasks, the attention module in the neural network structure, capturing temporal and spatial patterns, can be replaced by the simple MLP containing skip connection, layer normalization, and feedforward layers without significantly damaging the prediction performance. We have proposed an abstract structure for attention-based multivariate time series forecasting models by showing that the GCN modules to model spatial correlations are essentially modified attention mechanisms. With the proposed structure, we have demonstrated, empirically and theoretically, that the attention modules in the encoder structure are much less important than the ones in the decoder structure due to the greedy decoding mechanism.

The study has its limitations. Due to the vast majority of AMTSFM proposed, we cannot include all networks available for STF and LTSF tasks. Thus, some networks might require attention mechanisms to deliver their performance as

promised. Moreover, for both tasks, it takes researchers a great amount of effort to push the limit on forecasting accuracy forward by even a little. Therefore, it is worthwhile to stress that it is not our intention to render such hard work meaningless. Rather, we would like to help our fellow researchers distinguish the core contributor from the rest and offer insight into a new direction of forecasting networks. For future directions, we would like to propose the following: 1) discover the core contributor in the decoder structure; 2) ascertain if the results can be viewed in other tasks, such as computer vision and natural language process; 3) a metric to assess the effectiveness of the attention module for large language model pruning tasks.

Acknowledgments

References

[1] Elissaios Sarmas, Nikos Dimitropoulos, Vangelis Marinakis, Zoi Mylona, and Haris Doukas. Transfer learning strategies for solar power forecasting under data scarcity. *Sci Rep*, 12(1):14643, August 2022.

[2] Songgaojun Deng, Shusen Wang, Huzefa Rangwala, Lijing Wang, and Yue Ning. Cola-GNN: Cross-location attention based graph neural networks for long-term ILI prediction. In *CIKM*, CIKM '20, pages 245–254, New York, NY, USA, 2020. Association for Computing Machinery.

[3] Audeliano Wolian Li and Guilherme Sousa Bastos. Stock Market Forecasting Using Deep Learning and Technical Analysis: A Systematic Review. *IEEE Access*, 8:185232–185242, 2020.

[4] Zonghan Wu, Shirui Pan, Guodong Long, Jing Jiang, Xiaojun Chang, and Chengqi Zhang. Connecting the Dots: Multivariate Time Series Forecasting with Graph Neural Networks. In *SIGKDD*, KDD '20, pages 753–763. ACM, August 2020.

[5] Yi Zheng, Qi Liu, Enhong Chen, Yong Ge, and J. Leon Zhao. Time series classification using multi-channels deep convolutional neural networks. In Feifei Li, Guoliang Li, Seung-won Hwang, Bin Yao, and Zhenjie Zhang, editors, *WAIM*, volume 8485 of *Lecture Notes in Computer Science*, pages 298–310. Springer, 2014.

[6] Ailing Zeng, Muxi Chen, Lei Zhang, and Qiang Xu. Are transformers effective for time series forecasting? In *AAAI*, pages 11121–11128, Washington, DC, USA, 2023.

[7] Yuqi Nie, Nam H. Nguyen, Phanwadee Sinthong, and Jayant Kalagnanam. A time series is worth 64 words: Long-term forecasting with transformers. In *ICLR*. OpenReview.net, 2023.

[8] Haoyi Zhou, Shanghang Zhang, Jieqi Peng, Shuai Zhang, Jianxin Li, Hui Xiong, and Wancai Zhang. Informer: Beyond Efficient Transformer for Long Sequence Time-Series Forecasting. In *AAAI*, pages 11106–11115, 2021.

[9] Haixu Wu, Jiehui Xu, Jianmin Wang, and Mingsheng Long. Autoformer: Decomposition transformers with auto-correlation for long-term series forecasting. In M. Ranzato, A. Beygelzimer, Y. Dauphin, P.S. Liang, and J. Wortman Vaughan, editors, *NeurIPS*, volume 34, pages 22419–22430. Curran Associates, Inc., 2021.

[10] Shizhan Liu, Hang Yu, Cong Liao, Jianguo Li, Weiyao Lin, Alex X. Liu, and Schahram Dustdar. Pyraformer: Low-complexity pyramidal attention for long-range time series modeling and forecasting. In *ICLR*. OpenReview.net, 2022.

[11] Nikita Kitaev, Lukasz Kaiser, and Anselm Levskaya. Reformer: The efficient transformer. In *ICLR*. OpenReview.net, 2020.

[12] Sinong Wang, Belinda Z. Li, Madian Khabsa, Han Fang, and Hao Ma. Linformer: Self-attention with linear complexity. *CoRR*, abs/2006.04768, 2020.

[13] Feyza Duman Keles, Pruthuvi Mahesakya Wijewardena, and Chinmay Hegde. On the computational complexity of self-attention. In Shipra Agrawal and Francesco Orabona, editors, *ALT*, volume 201 of *Proceedings of Machine Learning Research*, pages 597–619. PMLR, 2023.

[14] Yong Liu, Tengge Hu, Haoran Zhang, Haixu Wu, Shiyu Wang, Lintao Ma, and Mingsheng Long. iTransformer: Inverted transformers are effective for time series forecasting. In *ICLR*. OpenReview.net, 2024.

[15] Gowtham Atluri, Anuj Karpatne, and Vipin Kumar. Spatio-temporal data mining: A survey of problems and methods. *ACM Comput. Surv.*, 51(4):83:1–83:41, 2018.

[16] Yaguang Li, Rose Yu, Cyrus Shahabi, and Yan Liu. Diffusion Convolutional Recurrent Neural Network: Data-Driven Traffic Forecasting. In *6th Int. Conf. Learn. Represent. ICLR*, February 2018.

[17] Bing Yu, Haoteng Yin, and Zhanxing Zhu. Spatio-temporal graph convolutional networks: A deep learning framework for traffic forecasting. In *Proc. Twenty-Seventh Int. Jt. Conf. Artif. Intell. IJCAI*, pages 3634–3640, 2018.

[18] Zonghan Wu, Shirui Pan, Guodong Long, Jing Jiang, and Chengqi Zhang. Graph WaveNet for Deep Spatial-Temporal Graph Modeling. In *Proc. Twenty-Eighth Int. Jt. Conf. Artif. Intell. IJCAI*, pages 1907–1913, 2019.

[19] JinHong Li, Jian Yang, Lei Gao, Lu Wei, and Fuqi Mao. Dynamic spatial-temporal graph convolutional GRU network for traffic forecasting. In *ICSCC*, pages 19–24. ACM, 2021.

[20] Chuanpan Zheng, Xiaoliang Fan, Cheng Wang, and Jianzhong Qi. GMAN: A Graph Multi-Attention Network for Traffic Prediction. In *Thirty-Fourth AAAI Conf. Artif. Intell. AAAI*, volume 34, pages 1234–1241, April 2020.

[21] Shengnan Guo, Youfang Lin, Huaiyu Wan, Xiucheng Li, and Gao Cong. Learning dynamics and heterogeneity of spatial-temporal graph data for traffic forecasting. *IEEE Trans. Knowl. Data Eng.*, 34(11):5415–5428, 2022.

[22] Chao Song, Youfang Lin, Shengnan Guo, and Huaiyu Wan. Spatial-temporal synchronous graph convolutional networks: A new framework for spatial-temporal network data forecasting. In *AAAI*, pages 914–921. AAAI Press, 2020.

[23] Haoyang Yan, Xiaolei Ma, and Ziyuan Pu. Learning dynamic and hierarchical traffic spatiotemporal features with transformer. *IEEE Trans. Intell. Transp. Syst.*, 23(11):22386–22399, 2022.

[24] Wenying Duan, Xiaoxi He, Zimu Zhou, Lothar Thiele, and Hong Rao. Localised adaptive spatial-temporal graph neural network. In Ambuj K. Singh, Yizhou Sun, Leman Akoglu, Dimitrios Gunopulos, Xifeng Yan, Ravi Kumar, Fatma Ozcan, and Jieping Ye, editors, *SIGKDD*, pages 448–458. ACM, 2023.

[25] Tianlong Chen, Yongduo Sui, Xuxi Chen, Aston Zhang, and Zhangyang Wang. A unified lottery ticket hypothesis for graph neural networks. In *ICML*, volume 139 of *Proceedings of Machine Learning Research*, pages 1695–1706. PMLR, 2021.

[26] Jiayu Li, Tianyun Zhang, Hao Tian, Shengmin Jin, Makan Fardad, and Reza Zafarani. SGCN: A graph sparsifier based on graph convolutional networks. In Hady W. Lauw, Raymond Chi-Wing Wong, Alexandros Ntoulas, Ee-Peng Lim, See-Kiong Ng, and Sinno Jialin Pan, editors, *PAKDD*, volume 12084 of *Lecture Notes in Computer Science*, pages 275–287. Springer, 2020.

[27] Haoran You, Zhihan Lu, Zijian Zhou, Yonggan Fu, and Yingyan Lin. Early-bird gcns: Graph-network co-optimization towards more efficient GCN training and inference via drawing early-bird lottery tickets. In *AAAI*, pages 8910–8918. AAAI Press, 2022.

[28] Cheng Zheng, Bo Zong, Wei Cheng, Dongjin Song, Jingchao Ni, Wenchao Yu, Haifeng Chen, and Wei Wang. Robust graph representation learning via neural sparsification. In *ICML*, volume 119 of *Proceedings of Machine Learning Research*, pages 11458–11468. PMLR, 2020.

[29] Jiawei Jiang, Chengkai Han, Wayne Xin Zhao, and Jingyuan Wang. PDFormer: Propagation delay-aware dynamic long-range transformer for traffic flow prediction. *CoRR*, abs/2301.07945, 2023.

[30] Hangchen Liu, Zheng Dong, Renhe Jiang, Jiewen Deng, Jinliang Deng, Quanjun Chen, and Xuan Song. STAEformer: Spatio-temporal adaptive embedding makes vanilla transformer SOTA for traffic forecasting. *CoRR*, abs/2308.10425, 2023.

[31] Shiyang Li, Xiaoyong Jin, Yao Xuan, Xiyou Zhou, Wenhu Chen, Yu-Xiang Wang, and Xifeng Yan. Enhancing the locality and breaking the memory bottleneck of transformer on time series forecasting. In Hanna M. Wallach, Hugo Larochelle, Alina Beygelzimer, Florence d'Alché-Buc, Emily B. Fox, and Roman Garnett, editors, *NeurIPS*, pages 5244–5254, 2019.

[32] Tian Zhou, Ziqing Ma, Qingsong Wen, Xue Wang, Liang Sun, and Rong Jin. FEDformer: Frequency enhanced decomposed transformer for long-term series forecasting. In Kamalika Chaudhuri, Stefanie Jegelka, Le Song, Csaba Szepesvári, Gang Niu, and Sivan Sabato, editors, *ICML*, volume 162 of *Proceedings of Machine Learning Research*, pages 27268–27286. PMLR, 2022.

[33] Ashish Vaswani, Noam Shazeer, Niki Parmar, Jakob Uszkoreit, Llion Jones, Aidan N. Gomez, Łukasz Kaiser, and Illia Polosukhin. Attention is all you need. In *Adv. Neural Inf. Process. Syst. 30 NeurIPS*, pages 5998–6008, Long Beach, CA, USA, 2017.

[34] Ruili Feng, Kecheng Zheng, Yukun Huang, Deli Zhao, Michael I. Jordan, and Zheng-Jun Zha. Rank diminishing in deep neural networks. In *NeurIPS*, 2022.

[35] Yihe Dong, Jean-Baptiste Cordonnier, and Andreas Loukas. Attention is not all you need: Pure attention loses rank doubly exponentially with depth. In Marina Meila and Tong Zhang, editors, *ICML*, volume 139 of *Proceedings of Machine Learning Research*, pages 2793–2803. PMLR, 2021.